Optical Property and Local Environment of Ni^{2+} in Fluoride Glasses

Hikari Shigemura,* Masanori Shojiya, Ryoji Kanno, and Yoji Kawamoto

Division of Molecular Science, Graduate School of Science and Technology, Kobe University, Nada, Kobe 657-8501, Japan

Kohei Kadono

Department of Optical Materials, Osaka National Research Institute, Ikeda, Osaka 563-8577, Japan

Masahide Takahashi

Venture Business Laboratory, Kobe University, Nada, Kobe 657-8501, Japan

Received: October 13, 1997; In Final Form: December 16, 1997

Optical absorption and extended X-ray absorption fine structure (EXAFS) spectra were measured on series of $ZrF_4-BaF_2-LaF_3$, $ZrF_4-BaF_2-MF-LaF_3$ (M; Li, Na, K, Rb, or Cs) and $AlF_3-BaF_2-CaF_2-YF_3$ glasses doped with Ni^{2+}. The optical absorption spectra show that Ni^{2+} ions in all the glasses exist in octahedral coordination sites with six F^- ions. The values of ligand field strength, $10Dq$, were obtained from the optical absorption spectra, and Ni−F interatomic distances, r_{Ni-F}, were determined by EXAFS analyses. The linear relationship between $10Dq$ and r_{Ni-F} is found and interpreted by simple ligand field theory. The compositional dependence of the $10Dq$ and r_{Ni-F} is discussed in terms of the basicity of glasses. We discuss the optical property and the local environment of Ni^{2+} in the fluoride glasses in comparison with those of oxide glasses.

Introduction

Glasses doped with 3d-transition metal ions and rare earth ions have been used as optical devices such as fiber amplifiers and fiber lasers. It is well-known that Er^{3+}-doped silica glass fiber has been practically used as a fiber amplifier operating at 1.5 μm. The absorption and emission bands in Cr^{3+}-doped glasses have been studied for applications to lasers around 1.0 μm.[1,2] The optical transition properties of these emission center ions in glasses are affected by coordination environments around them, i.e. bonding character and local structure including coordination number, bond distance, and bond angle. Therefore, the investigation of local environments around emission center ions is one of the most important subjects for systematically understanding optical properties of those ions.

The local environments of emission center ions in oxide glasses have been investigated in detail. A large number of studies using of ESR and optical absorption have been carried out in order to obtain information on the chemical bonding character of transition metal ions in glasses. The covalency of the Cu−O bond in Cu^{2+}-doped alkali silicate glasses has been studied by ESR.[3] The Ni−O bonding character has been discussed by optical absorption of Ni^{2+} in alkali borate glasses[4,5] and alkali silicate glasses[6] through ligand field theory and molecular orbital approach. Moreover, the local structure, i.e., the interatomic distance and coordination number concerning Ni^{2+} and Cu^{2+} ions in sodium borate glasses was revealed by EXAFS analyses.[7,8] Further, there are many investigations on the local environments of emission center ions in oxide glasses.

Recently, non-oxide glass systems have attracted much attention[9−11] because oxide glasses are insufficient as optical materials for all the kinds of devices. Fluoride glasses have been recognized as the majority of such new optical materials, because they have advantageous properties such as low phonon energy and excellent optical transparency extending from near UV to middle IR. A number of studies have provided optical properties of emission center ions in fluoride glasses. Optical absorption, emission, and lifetime have been investigated in fluorozirconate glasses doped with rare earth ions[12−16] of Tm^{3+}, Er^{3+}, and Nd^{3+} and with 3d-transition metal ions[17,18] of Ni^{2+}, Co^{2+}, and Mn^{2+}. However, the optical property is hardly investigated from the respect of local environment in fluoride glasses. Even the local environments of emission center ions in fluoride glasses have been scarcely researched. Only a Mössbauer study of Eu^{3+} and a series of ESR studies of several 3d-transition metal ions in fluoride glasses have been reported.[19−22]

In this study, the optical property and the local environment of Ni have been investigated in series of $ZrF_4-BaF_2-LaF_3$ (ZBL), $ZrF_4-BaF_2-MF-LaF_3$ (M; Li, Na, K, Rb or Cs) (ZBML), and $AlF_3-BaF_2-CaF_2-YF_3$ (ABCY) glasses in order to clarify the correlation between them. We selected Ni for a probe ion, because absorption spectra in many oxide glasses have shown that Ni ions always exist as divalent in the glasses and can be easily interpreted by their simple energy levels. In the fluoride glasses doped with Ni^{2+} ions, optical absorption was measured and ligand field strength was estimated from the transition energy of optical absorption. The Ni−F bonding character has been discussed through ligand field theory and molecular orbital approach. On the other hand, the local structure of Ni^{2+} ions in fluoride glasses was examined by EXAFS of the Ni K-edge. As the result, the relationship between the optical property and the local environment of Ni^{2+} has been discussed. Furthermore, the compositional dependence

* Corresponding author. Tel: +81-78-803 0593. Fax: +81-78-803-0722. E-mail: hikari@gradest2.scitec.kobe-u.ac.jp.

S1089-5647(97)03311-7 CCC: $15.00
Published on Web 02/24/1998

TABLE 1: Compositions of Prepared Fluoride Glasses

glass system	composition (mol %)
ZBL	$(95-x)ZrF_4 \cdot xBaF_2 \cdot (5-y)LaF_3 \cdot yNiF_2$
	$x = 20, 25, 30, 35, 40$ $y = 0.5, 3$
ABCY	$(84.5-x)AlF_3 \cdot x(0.5BaF_2 \cdot 0.5CaF_2) \cdot (15.5-y)YF_3 \cdot yNiF_2$
	$x = 37, 39.5, 42, 44.5, 47$ $y = 0.5, 1$
ZBML	$58.5ZrF_4 \cdot 31.5BaF_2 \cdot 5MF \cdot (5-y)LaF_3 \cdot yNiF_2$
	M = Li, Na, K, Rb, Cs $y = 0.5, 3$

of both ligand field strength and local structure of Ni^{2+} ions has been explained by the basicity of glasses. This is the first research, to our knowledge, that reveals that the optical property of 3d-transition metal ions in fluoride glasses can be related to their local environment.

Experimental Procedure

(a) Glass Preparation. The compositions of glasses used in the present study are listed in Table 1. Highly pure reagents of metal fluorides were used as raw materials for the preparation of glasses. About 5 g batches of the raw materials with the fluoridizing agent $NH_4F \cdot HF$ were melted at 450 °C for 15 min and subsequently at 950 °C for 15 min in a platinum crucible under argon gas atmosphere. The melts were cast into brass molds, which were kept at around 150−300 °C. The obtained glasses were annealed at their glass transition temperatures. The glasses containing 0.5 mol % NiF_2 were employed for optical absorption measurements, and those containing 1 or 3 mol % NiF_2 were for X-ray absorption measurements.

(b) Spectroscopic Measurements. Optical absorption spectra were measured in the wavelength range from 250 to 2500 nm at room temperature with Shimadzu UV-2200 and Hitachi 330 spectrophotometers.

X-ray absorption measurements were carried out at Beam Line 6B of the Photon Factory in the National Laboratory for High Energy Physics (KEK-PF).[23] The measurements were performed in transmission mode at the Ni K-edge around 8.3 keV. A monochromatic X-ray was obtained by a Si(111) two-crystal monochrometer. Different gasses were employed in the ionization chambers for detecting X-ray intensities before and after a sample. The spectra were obtained by averaging three measurements. The measurements for crystalline compounds of NiF_2 and $NaNiF_3$ were also performed under the same condition to obtain some parameters that are required for data analysis.

Results

(a) Optical Absorption. Figure 1 shows an optical absorption spectrum of Ni^{2+} ions in a ZBL glass as a function of wavenumber. The similar spectral feature was observed in all ZBL, ABCY, and ZBML glasses. It has been known that Ni^{2+} ions in glasses exist in either octahedral or tetrahedral coordination, which have quite different absorption characteristics from each other.[24,25] The inset of Figure 1 shows absorption spectra of Ni^{2+}-doped $CsMgCl_3$ and Cs_2MgCl_4 crystals,[26] in which Ni^{2+} is known to substitute for Mg^{2+} at the site of octahedral and tetrahedral symmetries, respectively. The absorption spectrum of Ni^{2+} in the glass has a profile similar to that in $CsMgCl_3$ crystal. This indicates that Ni^{2+} ions in the fluoride glasses are not in coordination of F^- tetrahedra but in coordination of F^- octahedra.

The absorption spectrum consists of three major bands labeled ν_1, ν_2, and ν_3 and two weak bands labeled ν_4 and ν_5. The bands are assigned to the transitions from $^3A_{2g}(F)$ of the ground state to $^3T_{2g}(F)$, $^3T_{1g}(F)$, $^3T_{1g}(P)$, $^1E_g(D)$, and $^1T_{2g}(D)$, respectively,

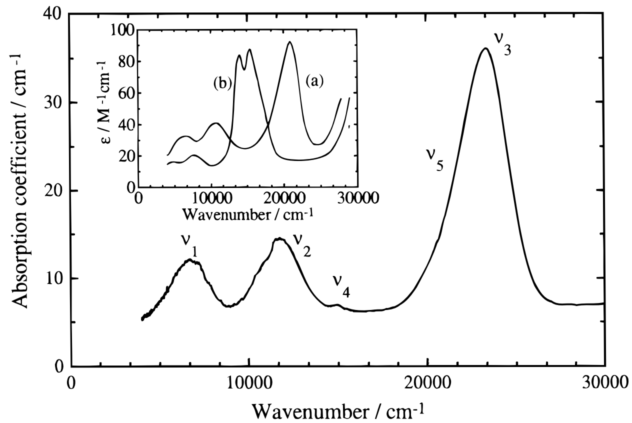

Figure 1. Optical absorption spectrum of Ni^{2+} in $75ZrF_4 \cdot 20BaF_2 \cdot 4.5LaF_3 \cdot 0.5NiF_2$ glass. The inset is absorption spectra of Ni^{2+} in (a) $CsMgCl_3$ and (b) Cs_2MgCl_4 crystals (ref 26). The vertical axis of the inset figure is expressed in molar absorptivity, ϵ.

TABLE 2: Peak Wavenumbers and Crystal Parameters of Ni^{2+} Ions in ZBL [$(95-x)ZrF_4 \cdot xBaF_2 \cdot 4.5LaF_3 \cdot 0.5NiF_2$], ABCY [$(84.5-x)AlF_3 \cdot x(0.5BaF_2 \cdot 0.5CaF_2) \cdot 15YF_3 \cdot 0.5NiF_2$], and ZBML [$58.5ZrF_4 \cdot 31.5BaF_2 \cdot 5MF \cdot 4.5LaF_3 \cdot 0.5NiF_2$] Glasses

	peak wavenumber (10^4 cm^{-1})					crystal parameter (10^3 cm^{-1})		
glass	ν_1	ν_2	ν_3	ν_4	ν_5	Dq	B	C
x in ZBL								
20	0.671	1.174	2.331	1.5	2.089	0.671	0.974	3.61
25	0.675	1.177	2.334	1.5	2.091	0.675	0.973	3.62
30	0.676	1.181	2.336	1.5	2.092	0.676	0.973	3.62
35	0.684	1.190	2.339	1.5	2.095	0.684	0.967	3.64
40	0.690	1.200	2.346	1.5	2.100	0.690	0.966	3.65
x in ABCY								
37	0.694	1.225	2.359	1.5	2.052	0.694	0.971	3.66
39.5	0.683	1.225	2.356	1.5	2.038	0.683	0.980	3.62
42	0.680	1.220	2.347	1.5	2.032	0.680	0.977	3.63
44.5	0.692	1.221	2.361	1.5	2.068	0.692	0.975	3.64
47	0.704	1.235	2.372	1.5	2.074	0.704	0.970	3.66
M in ZBML								
Li	0.679	1.221	2.345	1.5	2.036	0.679	0.976	3.64
Na	0.683	1.214	2.347	1.5	2.052	0.683	0.974	3.65
K	0.693	1.219	2.350	1.5	2.054	0.693	0.966	3.68
Rb	0.685	1.215	2.347	1.5	2.052	0.685	0.972	3.65
Cs	0.679	1.218	2.345	1.5	2.049	0.679	0.976	3.64

by referring to a previous work.[17] The wavenumbers of observed bands are given in Table 2. The mean wavenumber of each transition was adopted as the center of gravity of the absorption band. Overlapping bands were decomposed into Gaussian components. Table 2 also gives crystal field parameter, Dq, and Racah parameters, B and C, which describe electric interaction energies in the 3d shell. The Dq, B, and C parameters were obtained by applying the wavenumbers of ν_1, ν_3, and ν_4 bands to expressions given by solving the Tanabe−Sugano matrix;[27,28]

$$Dq = \frac{\nu_1}{10} \tag{1}$$

$$B = \frac{(\nu_3 - 2\nu_1)(\nu_3 - \nu_1)}{3(5\nu_3 - 9\nu_1)} \tag{2}$$

$$C = \frac{\nu_4}{2} - 5Dq - \frac{17}{4}B + \frac{1}{4}(400Dq^2 + 40DqB + 49B^2)^{1/2} \tag{3}$$

Accordingly, the ligand field strength, $10Dq$, of Ni^{2+} in octahedral symmetry was evaluated directly from the transition energy of the $^3A_{2g}(F) \rightarrow {}^3T_{2g}(F)$ band. The $10Dq$ of Ni^{2+} in

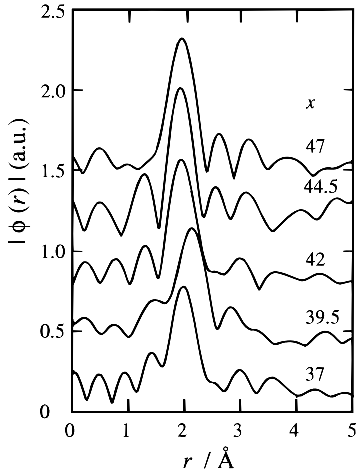

Figure 2. Fourier-transformed magnitudes of $k^3\chi(k)$, $|\phi(r)|$, obtained for $(84.5-x)AlF_3\cdot x\,(0.5BaF_2\cdot 0.5CaF_2)\cdot 14.5YF_3\cdot 1NiF_2$ glasses.

the fluoride glasses is found to be 6700−7000 cm^{-1}. In the ZBL system, the glass with higher BaF_2 content has larger 10*Dq* value. The 10*Dq* in the ABCY system does not change monotonously against (BaF_2 + CaF_2) content and has a minimum value at 39.5 mol %. In the ZBML system, the glass containing KF shows a maximum 10*Dq* value.

(b) Extended X-ray Absorption Fine Structure (EXAFS) Analysis. X-ray absorption spectra of glasses and reference compounds were analyzed by using the program package XAFSANAL.[29] The EXAFS oscillation, $\chi(k)$, is obtained as a function of photoelectron wave vector, k, after subtraction of smoothed X-ray absorption background and normalization by eq 4

$$\chi(k) = \frac{\mu(k) - \mu_0(k)}{\mu_0(k)} \quad (4)$$

where $\mu(k)$ is an X-ray absorption coefficient and $\mu_0(k)$ is that for the free atom.

The obtained k^3-weighted oscillation curves, $k^3\chi(k)$, were Fourier transformed over the range from 2.7 to 9.0 Å. The radial structural functions, $\phi(r)$, were obtained by Fourier transform of $k^3\chi(k)$. Figure 2 shows the Fourier-transformed magnitudes of $k^3\chi(k)$, $|\phi(r)|$, obtained for the ABCY glasses as an example. Inversely Fourier transformation was carried out for the main peak of $|\phi(r)|$. Then, the least-squares curve fitting was performed for the inversely Fourier-transformed spectra using the single scattering EXAFS formula,

$$k^3\chi(k) = \sum_j \frac{N_j k_j^{\,2}}{r_j^{\,2}} |f_j(k_j)| \exp(2\sigma_j^{\,2} k_j^{\,2} - 2r_j/\lambda_j) \sin[2k_j r_j + \delta_j(k_j)] \quad (5)$$

where N_j, r_j, σ_j, and λ_j are coordination number, interatomic distance, Debye−Waller type thermal parameter, and mean free path of the photoelectron of the jth coordination shell, respectively; $f_j(k)$ and $\delta_j(k)$ are theoretically calculated backscattering amplitude and total phase shift, respectively. Photoelectron wave vectors, k and k_j, are defined by

$$k = [2m/h^2(E - E^{\exp})]^{1/2} \quad (6)$$

$$k_j = [k^2 - 0.2625(\Delta E_j)]^{1/2} \quad (7)$$

TABLE 3: Structural Parameters of ZBL [$(95-x)ZrF_4\cdot xBaF_2\cdot 2LaF_3\cdot 3NiF_2$], ABCY [$(84.5-x)AlF_3\cdot x(0.5BaF_2\cdot 0.5CaF_2)\cdot 14.5YF_3\cdot 1NiF_2$], and ZBML [$58.5ZrF_4\cdot 31.5BaF_2\cdot 5MF\cdot 2LaF_3\cdot 3NiF_2$] Glasses Obtained by EXAFS Curve-Fitting

glass	r_{Ni-F} (Å) (±0.002 Å)	N_F (±2)	σ_F (Å) (±0.020 Å)
x in ZBL			
20	1.967	6.3	0.074
25	1.965	6.4	0.083
30	1.961	7.2	0.110
35	1.951	8.2	0.120
40	*a*	*a*	*a*
x in ABCY			
37	1.962	6.1	0.094
39.5	1.968	6.0	0.059
42	1.967	6.1	0.084
44.5	1.966	5.7	0.080
47	1.957	5.7	0.072
M in ZBML			
Li	1.967	6.0	0.082
Na	1.969	6.6	0.093
K	1.959	7.8	0.105
Rb	1.963	7.2	0.100
Cs	1.967	7.2	0.099

[a] Not available.

where m and h are the mass of the electron and Planck constant, respectively; E and $E^{\exp}$ are the X-ray photon energy and the experimental threshold energy. The threshold energy was determined from 8339.19 to 8339.57 eV. The ΔE_j is defined as the difference between $E^{\exp}$ and the theoretical threshold energy.[30] The curve-fitting analysis was performed from 4.0 to 8.0 Å^{-1} in the k range. In the curve-fitting for the glasses, the parameters except for r_j, N_j, and σ_j were fixed to the respective values resulting from curve-fitting for the reference compounds.

Table 3 gives the structural parameters of r_{Ni-F}, N_F, and σ_F obtained for the ZBL, ABCY, and ZBML glasses. Experimental errors were estimated as ±0.002 Å for the interatomic distance and ±2 for the coordination number. The Ni−F interatomic distance, r_{Ni-F}, varies from 1.95 to 1.97 Å with composition. These are smaller than the average r_{Ni-F} value in NiF_2 of the rutile structure (2.02 Å) and that in $NaNiF_3$ of the perovskite structure (1.97 Å). In the ZBL system, the glass with the higher BaF_2 content has a lower r_{Ni-F} value. In the ABCY system, the r_{Ni-F} value does not change monotonously against (BaF_2 + CaF_2) content and shows the maximum at 39.5 mol %. In the ZBML system, the glass containing KF shows the minimum r_{Ni-F} value. The coordination numbers, N_F, were in the range from 5.7 to 8.2. This is consistent with the result in optical absorption spectra, taking into account the experimental error of ±2.

Discussion

(a) Ligand Field Strength of Ni^{2+} in Glasses. The compositional dependence of 10*Dq* of Ni^{2+} in octahedral symmetry has been investigated in several oxide glass systems. Nelson et al. found that the 10*Dq* values of Ni^{2+} are constantly about 4800 cm^{-1} in a series of Na_2O-SiO_2 glasses.[6] Goto et al. revealed that the 10*Dq* of Ni^{2+} in $M_2O-B_2O_3$ (M: Li and Na) glasses varies widely from 5000 to 7500 cm^{-1}.[5] The 10*Dq* values of Ni^{2+} obtained in the present fluoride glasses are between 6700 and 7000 cm^{-1}. These values in the fluoride glasses are relatively larger than in the oxide glasses.

The ligand field strength of 3d-transition metal ions is generally related to the valency, coordination site, and electron-donating property which the ligand anions give to them in glasses. Since Ni ions in oxide and fluoride glasses are

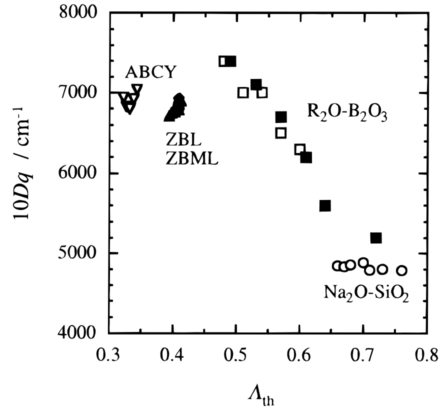

Figure 3. Relationship between $10Dq$ of Ni^{2+} and the theoretical basicity, Λ_{th}, in fluoride and oxide glasses: (▲) ZBL, (△) ZBML, (▽) ABCY, (■) $Na_2O-B_2O_3$ (ref 5), (□) $Li_2O-B_2O_3$ (ref 5), and (○) Na_2O-SiO_2 (ref 6).

constantly divalent and in octahedral coordination sites, the change of ligand field strength reflects the electron-donating property of ligand anions. Duffy and Ingram defined optical basicity of a glass as the electron-donating property of anions.[31−33] Theoretical basicity, Λ_{th}, defined by eq 8 is conveniently employed as the optical property, because it can be calculated from the glass composition,

$$\Lambda_{th} = \frac{x_{A^{a+}}}{\gamma_A} + \frac{x_{B^{b+}}}{\gamma_B} + \cdots \tag{8}$$

where $x_{A^{a+}}$, $x_{B^{b+}}$, ..., are the equivalent fractions of A^{a+}, B^{b+}, ..., and γ_A, γ_B, ..., are the corresponding moderating parameters. The moderating parameters are empirically represented by using the Pauling electronegativity, X, as follows;

$$\gamma_{(oxide)} = \frac{4X - 1}{3} \tag{9}$$

$$\gamma_{(fluoride)} = 2.3\gamma_{(oxide)} \tag{10}$$

The $10Dq$ values of Ni^{2+} in various glass systems are plotted against the theoretical basicity, Λ_{th}, in Figure 3. It is shown that the dependence of $10Dq$ on Λ_{th} is different in each glass system. The relationship between the $10Dq$ of Ni^{2+} and the basicity of glass can be explained by simple ligand field theory or molecular orbital approach.[24,25]

Simple ligand field theory considers interaction between d orbitals of Ni^{2+} and ligand anions. Applying this theory to glasses, ligand field strength monotonously increases with an increase in the basicity of the glass. However, as seen in Figure 3, the $10Dq$ decreases with increasing Λ_{th} in borate glasses and is nearly independent in sodium silicate glasses. Tanaka explains such a behavior of $10Dq$ in alkali borate glasses by the molecular orbital approach.[4] In the molecular orbital approach, Ni^{2+} and the ligand anion are considered as a set of molecular orbitals. Bonding orbitals to which 3d orbitals of the Ni^{2+} ion in the octahedron contribute consist of $\sigma(e_g)$ and $\pi(t_{2g})$ orbitals. Figure 4 shows a schematic illustration of the energy diagram for molecular orbitals of the Ni^{2+} ion and ligands in the octahedron. The separation between $\sigma^*(e_g^*)$ and π^* (t_{2g}^*) corresponds to ligand field strength. It is shown that d−pσ and d−pπ bondings give completely different effects on $10Dq$ values from each other; the former increases $10Dq$, while the latter decreases $10Dq$. This means that when the effect of d−pπ bondings on $10Dq$ is larger than that of d−pσ bondings, $10Dq$ should decrease with an increase in the basicity of the

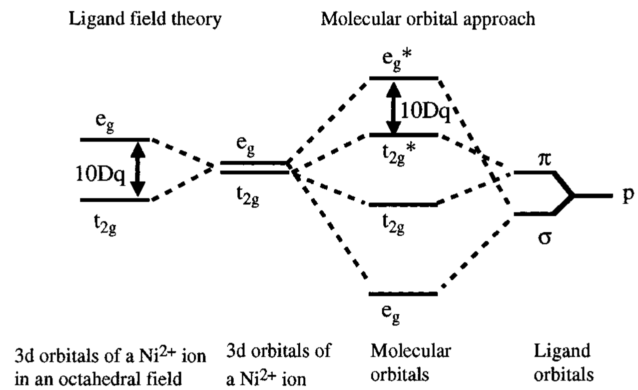

Figure 4. Energy level diagrams in the octahedral field of 3d orbitals of a Ni^{2+} ion and of molecular orbitals consisting of 3d orbitals of a Ni^{2+} ion and ligand orbitals.

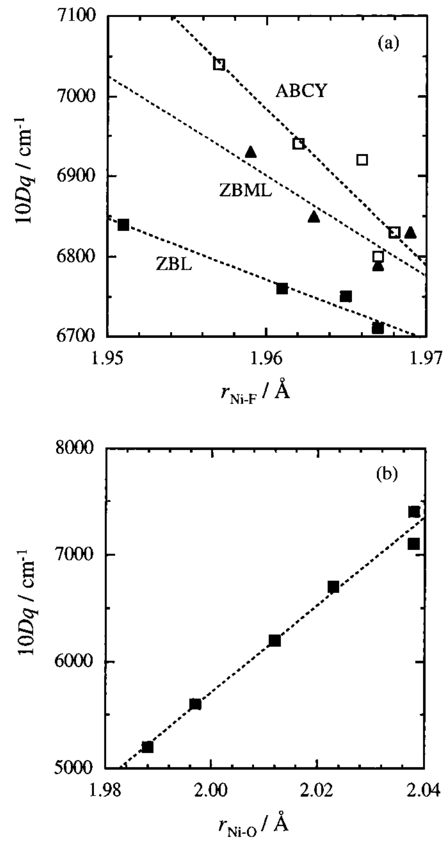

Figure 5. (a) $10Dq$ of Ni^{2+} as a function of Ni−F interatomic distance, r_{Ni-F}: (■) ZBL glasses, (□) ABCY glasses, (▲) ZBML glasses. (b) $10Dq$ of Ni^{2+} (ref 5) as a function of Ni−O interatomic distance, r_{Ni-O} (ref 7), in $Na_2O-B_2O_3$ glasses.

glass. Therefore, the behavior of $10Dq$ seen in alkali borate glasses is considered to be attributed to the variation of d−pπ bondings.

The $10Dq$ of Ni^{2+} in fluoride glasses obtained in the present study has various dependences upon the theoretical basicity; the $10Dq$ increases with increasing Λ_{th} in ZBL glasses and has a minimum in ABCY glasses. In ZBML glasses, the $10Dq$ varies in spite of a nearly constant Λ_{th} value. Here we obtain advanced insight into the local environment of Ni^{2+} from Ni−F interatomic distance, r_{Ni-F}. In the next section, we will discuss the relationship between $10Dq$ values of Ni^{2+} and Ni−F interatomic distances, r_{Ni-F}, and make clear the ligand field of Ni^{2+} in fluoride glasses.

(b) Relationship between 10*Dq* and r_{Ni-F}. In Figure 5a, the $10Dq$ values of Ni^{2+} are plotted against the corresponding

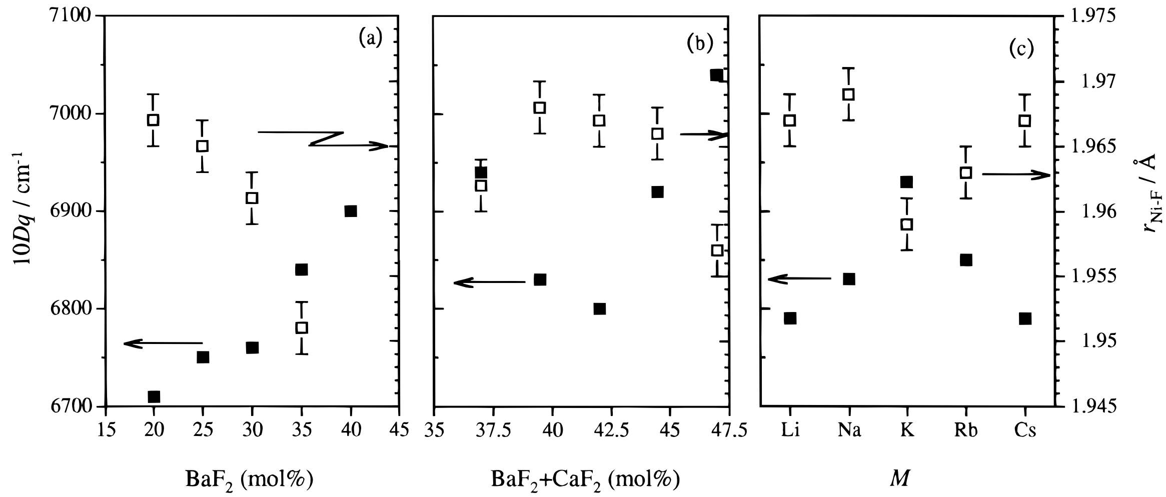

Figure 6. Ligand field strength, 10*Dq*, of Ni^{2+} and Ni−F interatomic distance, r_{Ni-F}, dependence on composition in (a) ZBL, (b) ABCY, and (c) ZBML glasses.

Ni−F interatomic distances, r_{Ni-F}, in ZBL, ABCY, and ZBML glasses. It is noteworthy that the 10*Dq* linearly increases with decreasing r_{Ni-F} in all the glass systems, even though the slopes are different from each other. A decrease in r_{Ni-F} is accompanied with increasing interaction between Ni and F through both σ bonding and π bonding. According to the molecular orbital approach, when the influence of σ bonding on 10*Dq* is more effective than that of π bonding, a decrease in r_{Ni-F} should increase 10*Dq*. When that of π bonding is more effective, a decrease in r_{Ni-F} should decrease 10*Dq*. Therefore, the behavior of r_{Ni-F} and 10*Dq* seen in Figure 5a indicates that σ-bonding character is more effective on the10*Dq* value of Ni^{2+} in fluoride glasses. This also suggests that the 10*Dq* value of Ni^{2+} in fluoride glasses can be interpreted by simple ligand field theory.

On the other hand, a quite different behavior can be seen in sodium borate glasses. Figure 5b shows the relationship between 10*Dq* of Ni^{2+} and Ni−O interatomic distance, r_{Ni-O} in $(100-x)B_2O_3 \cdot xNa_2O$ ($x = 10$, 15, 20, 25, 30, and 40). The 10*Dq* values in the glasses were cited from Goto et al.[5] The r_{Ni-O} values were cited from the EXAFS study by Xu et al.[7] These two studies were performed independently on glasses with the same composition. In contrast to the fluoride glasses, the 10*Dq* of Ni^{2+} decreases with decreasing of r_{Ni-O}, in this series of glasses. This proves that the influence of π bonding has more effect on the 10*Dq* in alkali borate glasses than that of σ bonding, which has been mentioned by Tanaka.[4]

It is clarified that 10*Dq* values of Ni^{2+} in the fluoride glasses are dominated by σ-bonding character in Ni−F bonding, while 10*Dq* values in the oxide glasses are dominated by π-bonding character in Ni−O bonding. This clearly reveals that the optical property of emission center ions depends on not only the local structure but the bonding character which is given by the host glasses.

(c) Compositional Dependence of 10*Dq* and Local Environment of Ni^{2+} in Fluoride Glasses. It is mentioned above that the local environment of Ni^{2+} in fluoride glasses can be dealt with by simple ligand field theory. Hence, we discuss results on the basis of simple ligand field theory in this section. Figure 6a presents both the ligand field strength, 10*Dq*, and the Ni−F interatomic distance, r_{Ni-F}, as a function of BaF_2 content in the ZBL glasses. It is shown that the 10*Dq* increases and the r_{Ni-F} decreases with BaF_2 content. The theoretical basicity of glasses increases with BaF_2 content. Since Ni−F interaction increases with increasing theoretical basicity of glass, according to ligand field theory, the 10*Dq* should increase and simultaneously r_{Ni-F} should decrease with BaF_2 content. Thus, it is proved that the changes in 10*Dq* and r_{Ni-F} can be explained by the basicity in ZBL glasses.

Figure 6b shows the dependence of 10*Dq* and r_{Ni-F} on (BaF_2 + CaF_2) content in ABCY glasses. It is interesting that the compositional dependence of 10*Dq* and r_{Ni-F} in the ABCY system is different from that in the ZBL system. Namely, there is no linear relationship between 10*Dq* and (BaF_2 + CaF_2) content. On the basis of the result in the ZBL system, 10*Dq* should increase with increasing (BaF_2 + CaF_2) content, because the theoretical basicity of the glass increases with alkaline earth content. The 10*Dq*, however, decreases in the part of lower alkaline earth content. This suggests that the basicity of the glasses with lower alkaline earth content cannot be estimated from the theoretical basicity. The theoretical basicity is calculated from the glass composition and hence cannot be estimated if significant structural changes occur with alkaline earth content in the glass. Therefore we consider that this behavior of 10*Dq* arises from some structural change in the glasses. It is noted here that the Raman spectroscopic study of AlF_3−BaF_2−CaF_2 glasses also suggests the structural changes in bridging of AlF_6 structural units.[34] Further work is under way to clarify this phenomenon.

The 10*Dq* and r_{Ni-F} are plotted against the glass-modifying alkali component in ZBML glasses in Figure 6c. It is shown that 10*Dq* has the maximum value at the glass containing K^+ and decreases in the order of Na^+ and Li^+ and also in the order of Rb^+ and Cs^+. The 10*Dq* and r_{Ni-F} remarkably change in ZBML glasses as much as in ZBL and ABCY glass systems, although alkali fluoride is only 5 mol %. This suggests that local structure around Ni^{2+} is much affected by alkali cations in the fluoride glasses.

Conclusions

Optical absorption and X-ray absorption were measured for Ni^{2+}-doped ZrF_4-based and AlF_3-based glasses. Ni^{2+} ions in the fluoride glasses exist in coordination of F^- octahedra, regardless of glass composition. It was found that the ligand field strength, 10*Dq*, linearly increases with decreasing Ni−F interatomic distance, r_{Ni-F}, in the fluoride glasses. This indicates that σ-bonding character is more effective on the 10*Dq* value in the fluoride glasses, although π-bonding character is more effective in oxide glasses. Further, we discussed glass compositional dependence of 10*Dq* and r_{Ni-F} in terms of basicity of glasses. The 10*Dq* increases and r_{Ni-F} decreases with the theoretical basicity in the ZrF_4-based glasses. This is explained by simple ligand field theory. The changes in 10*Dq* and r_{Ni-F} by various alkali components in ZrF_4-based glasses suggest that the local structure around Ni^{2+} is largely affected by alkali cations. In the AlF_3-based glasses, the dependence of 10*Dq* and r_{Ni-F} on ($BaF_2 + CaF_2$) content suggests that some structural changes in the linkage of AlF_6 structural unit occurs with the content.

Acknowledgment. The authors are grateful to the Photon Factory in the National Laboratory for High Energy Physics (KEK-PF) for providing us with the experimental opportunity (92-X019).

References and Notes

(1) Balada, R.; Fernández, J.; Illarramendi, M. A. *J. Phys.: Condens. Matter* **1992**, *4*, 10323.
(2) Balada, R.; et al. *Phys. Rev. B* **1991**, *44*, 4759.
(3) Hosono, H.; Kawazoe, H.; Kanazawa, T. *J. Non-Cryst. Solid* **1979**, *33*, 103.
(4) Tanaka, K.; Hirao, K.; Soga, N. *Phys. Chem. Glasses* **1993**, *34*, 127.
(5) Goto, Y.; Osaka, A.; Takahashi, K. *Yogyo-Kyokaishi* **1972**, *80*, 17.
(6) Nelson, C.; White, W. B. *Phys. Chem. Glasses* **1993**, *34,* 219.
(7) Xu, Q.; Maekawa, T.; Kawamura, K.; Yokokawa, T. *Phys. Chem. Glasses* **1990**, *31*, 151.
(8) Xu, Q.; Maekawa, T.; Kawamura, K.; Yokokawa, T. *Phys. Chem. Glasses* **1990**, *31*, 10.
(9) Shojiya, M.; et al. *Appl. Phys. Lett*. **1994**, *65*, 1874.
(10) Shojiya, M.; et al. *Appl. Phys. Lett*. **1995**, *67*, 2453.
(11) Kadono, K.; et al. *J. Non-Cryst. Solid* **1995**, *184*, 309.
(12) Tanabe, S.; Hanada, T. *J. Appl. Phys*. **1994**, *76*, 3730.
(13) Takahashi, M.; et al. *J. Non-Cryst. Solid* **1994**, *168*, 137.
(14) Takahashi, M.; et al. *Mater. Res. Bull*. **1993**, 28, 557.
(15) Takahashi, M.; et al. *J. Appl. Phys*. **1997**, *81*, 2940.
(16) Ohishi, Y.; Kanamori, T.; Nishi, T.; Takahashi, S. *IEEE Photo. Lett*. **1991**, *3*, 715.
(17) Suzuki, Y.; et al. *Phys. Rev. B* **1987**, *35*, 4472.
(18) Ohishi, Y.; Mitachi, S.; Kanamori, T.; Manabe, T. *Phys. Chem. Glasses* **1983**, *24*, 135.
(19) Takahashi, M.; Kanno, R.; Kawamoto, Y. *J. Phys. Chem*. **1996**, *100*, 11193.
(20) Legein, C.; Buzaré, J. Y.; Jacoboni, C.; *J. Non-Cryst. Solids* **1993**, *161*, 112.
(21) Legein, C.; Buzaré, J. Y.; Emery, J.; Jacoboni, C. *J. Phys.: Condens. Matter* **1995**, *7*, 3853.
(22) Legein, C.; Buzaré, J. Y.; Boulard, B.; Jacoboni, C. *J. Phys.: Condens. Matter* **1995**, *7*, 4829.
(23) Nomura, M.; Koyama, A. In *X-ray Absorption Fine Structure*; Hasnain, S. S., Ed.; Ellis Horwood: London, 1991; p 667.
(24) Sutton, D. *Electronic Spectra of Transition Metal Complexes*; McGraw-Hill Publishing Co. Ltd.: New York, 1968; p 117.
(25) Bates, T. *Modern Aspects of the Vitreous State*; Mackenzie, J. M., Ed.; Butterworth: London, 1962; Vol. 2, p 195.
(26) Angel, C. A.; Gruen, D. M. *J. Phys. Chem*. **1966**, *70*, 1601.
(27) Tanabe, Y.; Sugano, S. *J. Phys. Soc. Jpn.* **1954**, *9*, 735.
(28) Tanabe, Y.; Sugano, S. *J. Phys. Soc. Jpn.* **1954**, *9*, 766.
(29) Sakane, H. *Ph.D. Thesis, Osaka University*, 1991. The main parts of the programs used in these analyses were XASANAL, FTRANS, FFILTER, and CFL.
(30) Teo, B. K. *EXAFS: Basic Principles and Data Analysis*; Springer-Verlag: Berlin, 1986; p 288.
(31) Duffy, J. A.; Ingram, M. D. *J. Non-Cryst. Solids* **1976**, *21*, 373.
(32) Duffy, J. A. *J. Non-Cryst. Solids* **1989**, *109*, 35.
(33) Duffy, J. A.; Ingram, M. D. *J. Non-Cryst. Solids* **1992**, *144*, 76.
(34) Kawamoto, Y.; Kono, A. *J. Non-Cryst. Solids* **1986**, *85*, 335.